Joint Diseases and Related Surgery

Jt Dis Relat Surg
2025;36(2):328-339

ORIGINAL ARTICLE

Irisin and its role in fracture healing: A comparative study with hyaluronic acid and platelet-rich plasma in a rat model

Ahmet Emrah Açan, MD[1], Mert Emre Aydın, MD[1], Özgür Bulmuş, MD[2], Emrah Özcan, MD[3], Aslı Karakılıç, MD[2], Gülay Turan, MD[4], Reşit Buğra Hüsemoğlu, MSc[5]

[1]Department of Orthopedics and Traumatology, Balıkesir University Faculty of Medicine, Balıkesir, Türkiye
[2]Department of Physiology, Balıkesir University Faculty of Medicine, Balıkesir, Türkiye
[3]Department of Anatomy, Balıkesir University Faculty of Medicine, Balıkesir, Türkiye
[4]Department of Pathology, Balıkesir University Faculty of Medicine, Balıkesir, Türkiye
[5]Department of Biomechanics, Dokuz Eylül University Institute of Health Sciences, İzmir, Türkiye

Fracture healing is one of the oldest topics in orthopedic practice and remains a challenge due to delayed union and nonunion. This issue is further exacerbated by aging populations and associated socioeconomic burdens, with nonunion rates ranging from 2 to 30% despite advancements in treatment.[1,2] Therefore, most studies addressing into improvement of the fracture healing remain consistently relevant and of ongoing importance.[3-6]

Platelet-rich plasma (PRP) contains growth and differentiation factors such as platelet-derived growth factor (PDGF), insulin-like growth factor 1 (IGF-1), IGF-2, tumor growth factor-beta (TGF-β), vascular endothelial growth factor (VEGF), and

Received: December 05, 2024
Accepted: February 09, 2025
Published online: April 05, 2025

Correspondence: Ahmet Emrah Açan, MD. Balıkesir Üniversitesi Tıp Fakültesi, Ortopedi ve Travmatoloji Anabilim Dalı, 10185 Altıeylül, Balıkesir, Türkiye.

E-mail: dremrahacan@hotmail.com

Doi: 10.52312/jdrs.2025.2097

Citation: Açan AE, Aydın ME, Bulmuş Ö, Özcan E, Karakılıç A, Turan G, et al. Irisin and its role in fracture healing: A comparative study with hyaluronic acid and platelet-rich plasma in a rat model. Jt Dis Relat Surg 2025;36(2):328-339. doi: 10.52312/jdrs.2025.2097.

ABSTRACT

Objectives: This study aims to investigate the effects of local irisin (IR) injections on closed femoral fractures in rats and to compare its efficacy to platelet-rich plasma (PRP) and hyaluronic acid (HA).

Materials and methods: A total of 64 male Wistar albino rats were divided into four equal groups: a control group that received no treatment and three experimental groups that received local injections of HA, PRP, or recombinant IR at the fracture site. All rats underwent a standard bilateral closed femoral shaft fracture and intramedullary fixation. Each group was further divided into two subgroups, sacrificed at Week 2 and Week 4. The right femurs were used for radiological examination with micro-computed tomography (micro-CT) and subsequent histological analysis, while the left femurs were reserved for biomechanical testing.

Results: By Week 2, the IR and PRP groups showed statistically significantly higher scores for the transformation of fibrous cartilage into bone tissue compared to the control group (7.88±0.6, p=0.0001, and 6±0.8, p=0.036, respectively). By Week 4, transformation scores in the IR group increased to 9.25±0.7, statistically significantly exceeding the control group (p=0.0001). Bone volume was also statistically significantly greater in the IR group (5.21±0.5 mm^3 at Week 2; 5.94±0.8 mm^3 at Week 4) compared to the control group (p=0.001) and the PRP group (p=0.003) at Week 2, and compared to the control group (p=0.001), the HA group (p=0.042), and the PRP group (p=0.014) at Week 4. Additionally, maximum strength in the IR group was statistically significantly higher than in the control group (p=0.0001) and the PRP group (p=0.048) at Week 2. By Week 4, the IR group was also statistically significantly higher compared to the control group (p=0.0001), the HA group (p=0.037) and the PRP group (p=0.009).

Conclusion: The present study is one of the first to demonstrate the potential of administering local IR via injection into the fracture hematoma to accelerate fracture healing. The superior efficacy of IR over HA and PRP may be explained by its ability to enhance osteoblast activity, promote vascularization, and reduce inflammation, creating an optimal environment for bone regeneration. Unlike PRP, which primarily delivers growth factors, and HA, which supports cell migration and proliferation, IR appears to directly influence the bone microenvironment, expediting callus transformation. These findings suggest that IR may play a significant role in improving outcomes for patients at risk of delayed union. However, further clinical trials in humans are necessary to confirm its efficacy and safety for clinical applications.

Keywords: Fracture, healing, hyaluronic acid, irisin; platelet-rich plasma.

fibroblast growth factor (FGF). It is widely used in the treatment of tendinopathies, chondropathies, osteoarthritis, and muscle injuries, as well as in managing fractures and nonunions.[7-9] Similarly, hyaluronic acid (HA) enhances the activity of multiple cytokines and growth factors, particularly FGF-2 and VEGF, thereby promoting the formation of both soft and hard callus, facilitating cell migration, and aiding granulation tissue organization. Although its direct mitogenic activity has yet to be definitively established, HA significantly contributes to cell proliferation indirectly.[10,11]

Irisin (IR), discovered by Boström et al.[12] in 2012, is a myokine secreted into the blood by skeletal muscles following physical exercise. Initially, its effects were described in relation to adipose tissue and thermogenesis, and later in connection with metabolic diseases, Alzheimer's disease, and brain functions.[13,14] In the following years, the literature includes both *in vitro* and *in vivo* studies highlighting the anabolic effects of IR on bone cells and cartilage cells, with its potential to prevent the development of osteoporosis and osteoarthritis.[15-20]

Recently, only a limited number of studies have investigated the effects of IR on fracture healing.[21-26] In these experimental studies, recombinant IR has been administered to mice or rats either systemically through intraperitoneal injection or locally via various scaffolds or hydrogels. While previous studies have explored the systemic and scaffold-based local applications of IR, its direct local injection into the fracture hematoma still remains unexplored. This approach preserves the hematoma, a crucial element for fracture healing, and offers a minimally invasive alternative. In the present study, we aimed to evaluate the effects of local recombinant IR injection into fracture hematoma in a closed femur shaft fracture model in rats and compare its efficacy with previously reported local applications of PRP and HA.

MATERIALS AND METHODS

This study was approved by the Balıkesir University Animal Ethics Committee (date: 28.09.2023, no: 2023/8-4). It involved 64 male Wistar albino rats (14 to 16 weeks old) housed at our university's animal research center. All procedures involving animals were conducted in accordance with the National Institutes of Health (NIH) Guide for the Care and Use of Laboratory Animals and adhered to international guidelines on animal research ethics.

Using G*Power software (effect size: 0.40, confidence level: 0.90, power: 0.80), the minimum number of rats required was calculated as 60. To ensure equal group distribution and account for potential dropouts, the study was conducted with 64 rats. The rats were randomly divided into four groups, and each group was further divided into two subgroups, with eight rats in each subgroup. The remaining four rats were reserved for PRP preparation. The groups were formed as follows: Group 1, the control group, underwent only closed femoral shaft fracture and intramedullary fixation. Groups 2, 3, and 4 received local injections of 0.1 mL of HA, PRP, and recombinant IR, respectively, using a 27-gauge insulin syringe. These groups were, then, subdivided based on the sacrificial time points, at Weeks 2 and 4. The procedures were performed bilaterally on each rat's femurs: the right femurs were designated for radiological examination using micro-computed tomography (micro-CT), followed by histological analysis, while the left femurs were reserved for biomechanical testing. The inclusion criterion for this study was the presence of mid-diaphyseal, non-comminuted closed femoral fractures. Exclusion criteria were as follows: rats that did not have mid-diaphyseal closed femoral fractures, as confirmed via palpation and radiological evaluation, or those that did not remain healthy until sacrification due to infection at the surgical site or significant weight loss. If any rat needed to be excluded due to exclusion criteria or death, replacement rats were planned to be randomized into the study using a drawing lots method to maintain equal group sizes and preserve the randomization integrity.

Surgical procedure and experimental design

Under anesthesia (80 mg/kg ketamine and 8 mg/kg xylazine, intraperitoneally), the right knee joint was shaved and covered with a sterile drape. Following this, an arthrotomy was performed using a medial parapatellar approach to the right knee. With the aid of a drill motor, a 1.0-mm Kirschner wire (K-wire) was advanced retrogradely from the intercondylar area of the femur to the trochanteric region. The wire was then withdrawn, and a closed fracture was created at the midshaft of the femur using the three-point bending technique described by Bonnarens and Einhorn.[27] After creating the fracture using this technique, the same individual checked through palpation whether the fracture was at the diaphyseal level and whether there

was any comminution. Afterward, the withdrawn K-wire was reinserted retrogradely and anchored at the greater trochanter (Figure 1). At the knee region, the wire was trimmed at the condyle to avoid restricting joint movement. Finally, the patella was reduced, and the medial parapatellar approach was sutured. On postoperative Day 0, while anesthesia was still ongoing, the same surgeon administered the treatments percutaneously into the fracture line using an insulin syringe with a 27-gauge needle. The correct positioning of the needle was confirmed by the tactile feedback of the needle entering the fracture line, ensuring precise delivery of the treatment. In Group 2, 3 and 4, 0.1 mL of HA, PRP, and recombinant IR protein was administered, respectively. All surgical procedures performed on the right side of the rat, as described previously, were repeated on the left side, performing bilateral femur fractures. Bilateral femur fractures were chosen to reduce the number of rats required for

FIGURE 1. (a) Arthrotomy performed using a medial parapatellar approach. **(b)** A 1.0 mm diameter Kirschner wire was advanced retrogradely from the intercondylar area of the femur to the trochanteric region. **(c)** The wire was then withdrawn, and a closed fracture was created at the midshaft of the femur using the three-point bending technique described by Bonnarens and Einhorn.[27] **(d)** The withdrawn Kirschner wire was reinserted retrogradely and trimmed at the condyle. Finally, the patella was reduced, and the layers was sutured.

the study and also ensure comparable testing conditions between radiological, histological, and biomechanical analyses, thereby minimizing inter-animal variability and enhancing the consistency of our results.

To ensure consistency in the experimental setup, the same injection volume (0.1 mL) was used for all groups. The dosages of HA and PRP were selected based on products routinely used in clinical practice. Hyaluronic acid (Regenflex Bioplus®, Regenyal S.r.l., San Benedetto del Tronto, Italy) was a commercially available product with a formulation containing two different fractions: a cross-linked HA with a high-molecular-weight ranging from 1 to 2 million Da and a linear fraction with a lower molecular weight of 500 KDa at a concentration of 25 mg/mL. Similarly, PRP was prepared using Easy PRP® Kit (Neotec Biotechnology, İstanbul, Türkiye), a product widely adopted in clinical settings. For PRP preparation, four donor rats were euthanized via intracardiac puncture after being anesthetized, with each donor providing sufficient PRP for the immediate treatment of four experimental rats. Considering that each surgical procedure took approximately 10 to 15 min, this approach ensured that PRP injections were administered within the optimal 1-h window, maintaining its freshness and efficacy. Approximately 5 mL of blood was drawn from each rat into tubes (Easy PRP® Kit, Neotec Biotechnology, Istanbul, Türkiye) containing 0.5 mL of citrate-phosphate-dextrose (CPD) as an anticoagulant. The samples were, then, centrifuged at 1,200 rpm for 10 min at room temperature to separate plasma from the cellular components. The upper plasma layer was collected and subjected to a second centrifugation at 2,000 rpm for 10 min to concentrate platelets. The resulting PRP was carefully separated, and the final volume was approximately 1 mL. This PRP was used within 1 h of preparation without further activation. The recombinant IR dosage was prepared as follows: a 100 μg IR vial (r-irisin; #11451: Cayman Chemicals; Ann Arbor, MI) was diluted with deionized water to a total volume of 10 mL. This resulted in a concentration of 10 μg/mL, and 100 μL were injected. The chosen IR dose was based on the study by Serbest et al.,[28] which evaluated serum IR concentrations in fracture patients.

Following the surgery, the rats' movements were not restricted, and no immobilization of their lower limbs was applied. The animals were housed in standard laboratory cages (four rats per cage) under controlled conditions, with a temperature of 22±2°C, a relative humidity of 50 to 60%, and a 12-h light/dark cycle. They had unrestricted access to standard pellet feed and water throughout the study until the sacrification, which was performed via cervical dislocation under high-dose anesthesia to minimize pain and distress. For each group, the first subgroup was sacrificed at Week 2, while the second subgroup was sacrificed at Week 4. The entire femur, including the fracture site with callus tissue, was carefully extracted from the hip and knee joint. Then, the K-wire was withdrawn from the trochlear entry point. The right femurs were sampled for radiological examination using micro-CT, followed by histological analysis, while the left femurs were sampled for biomechanical testing.

Radiological imaging

The femurs of the rats were preserved in a 10% formaldehyde solution until they were transported for micro-CT analysis. Micro-CT scans were conducted by positioning the femurs in a plastic holder and scanning them at a dose of 50 kVp and 45 mA, with a steep angle of 0.75 degrees and a length of 40 ms for each projection using a U-CT (MILabs MicroCT-OI). The scanned sections were reconstructed with voxel sizes of 60 μm. Following reconstruction in the coronal, sagittal and three-dimensional (3D) formats, the callus volume, bone volume and the callus volume/bone volume, were measured using an open-source software 3D Slicer (https://www.slicer.org/, version 5.7.0) (Figure 2).

Histological evaluation

After micro-CT scanning and the following two days of 10% formalin fixation, each sample was placed in a 10% ethylenediaminetetraacetic acid (EDTA) solution, which was refreshed every two days during the four-week decalcification period. The decalcified samples were embedded in paraffin and sliced into 5-micron thick sections. After deparaffinization, the tissue sections were stained with hematoxylin and eosin (Figure 3). Subsequently, a blinded pathologist performed a histological evaluation of healing at the fracture site according to the healing scale by Huo et al.,[29] which ranges from 0 (healing) to 10 (complete bony healing) (Table I).

Biomechanical testing

Rat femur bones were thawed at 4°C overnight and maintained at room temperature, wrapped in saline, prior to testing. Before conducting the biomechanical tests, the K-wires were carefully

removed. No complications, such as additional fractures or bone damage, were observed during the removal process. All tests were performed under bending load using an electromechanical actuator (5 kN AG-X; Shimadzu, Kyoto, Japan). The load (N) and displacement (mm) values obtained during the tests were simultaneously recorded by the tester's own software. A three-point bending model was designed to assess the distribution of the load encountered by the rat femur on the sagittal plane and extensional stability. The upper loading device was aligned with the center of the femoral shaft, while the lower device's two sides were placed on the support fixture, adjusting the

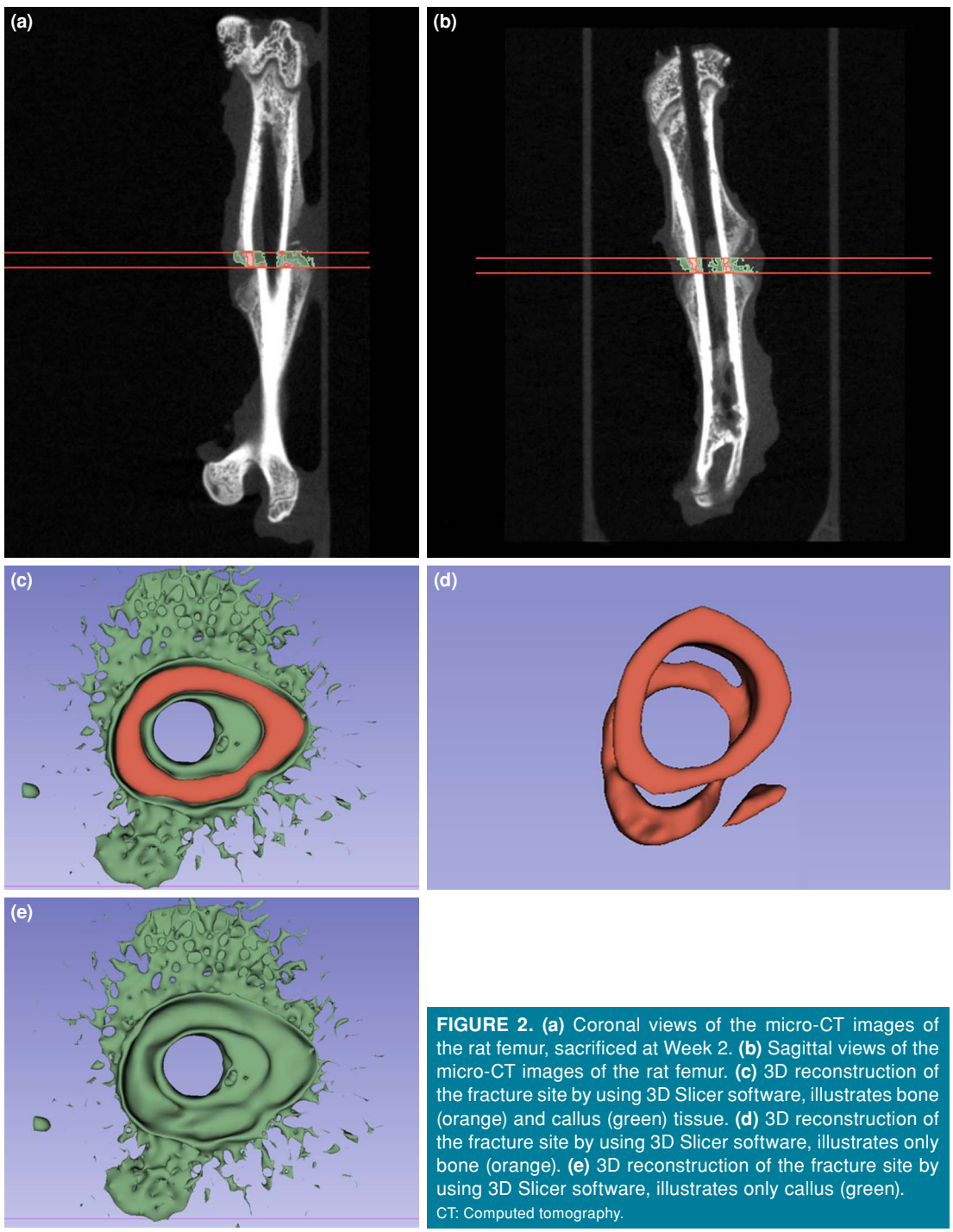

FIGURE 2. (a) Coronal views of the micro-CT images of the rat femur, sacrificed at Week 2. **(b)** Sagittal views of the micro-CT images of the rat femur. **(c)** 3D reconstruction of the fracture site by using 3D Slicer software, illustrates bone (orange) and callus (green) tissue. **(d)** 3D reconstruction of the fracture site by using 3D Slicer software, illustrates only bone (orange). **(e)** 3D reconstruction of the fracture site by using 3D Slicer software, illustrates only callus (green).
CT: Computed tomography.

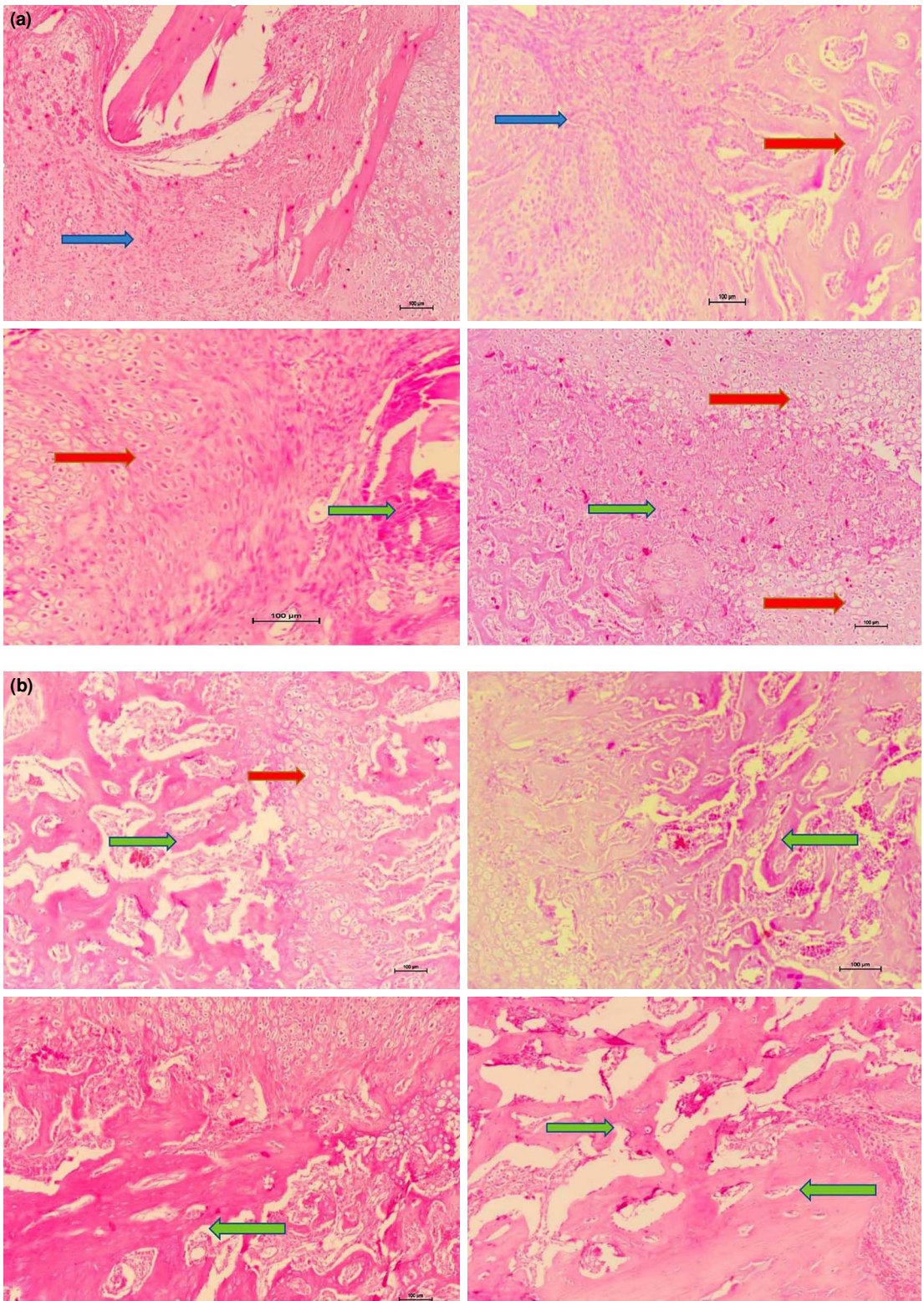

FIGURE 3. (a) The histologic images (H&E, ×200) correspond, from left to right, to the Control, HA, PRP and IR groups at Week 2, respectively. In the figure, the green, red, and blue arrows indicate bone tissue, cartilage tissue, and fibrosis, respectively. **(b)** The histological images (H&E, ×200) correspond to the Control, HA, PRP, and IR groups at Week 4, respectively, from left to right. In the figure, the green, red, and blue arrows indicate bone tissue, cartilage tissue, and fibrosis, respectively.

HA: Hyaluronic acid; PRP: Platelet-rich plasma; IR: Irisin.

span distance between the supports to 20 mm. Each test was performed at a speed of 5 mm/min until failure, and displacement versus load values were recorded.

Statistical analysis

Statistical analysis was performed using the IBM SPSS version 25.0 software (IBM Corp., Armonk, NY, USA). Descriptive data were expressed in mean ± standard deviation (SD), median (min-max) or number and frequency, where applicable. Comparisons among the averages of the groups were performed using the Kruskal-Wallis and pairwise comparison tests. A p value of <0.05 was considered statistically significant.

RESULTS

One rat in the PRP subgroup, scheduled for sacrifice at the fourth week, died the day after surgery. Five rats were excluded from the study, as, upon palpation of the fracture line after fracture creation, comminution was suspected, and those procedures were repeated with additional new rats. Following the exclusions, the study groups were complemented with replacement rats, resulting in a total of 64 rats included in the final analyses.

Histological findings

At Week 2, the mean transformation levels of fibrous cartilage into bone tissue were recorded as 1±0.0 in the control group, 5.88±0.8 in the HA group, 6±0.8 in the PRP group, and 7.88±0.6 in the IR group. The transformation levels in the IR and PRP groups were significantly higher compared to the control group, with p=0.0001 and p=0.036, respectively. By Week 4, these levels increased in each group, with mean values of 7.13±0.6, 8.13±0.6, 7.86±0.7, and 9.25±0.7, respectively. Remarkably, callus transformation scores of 10, indicating complete bone maturation, were observed only in the IR group (3 out of 8 specimens) at Week 4. However, the level of significance between the control and IR groups remained consistent at Week 4 (p=0.0001) (Figure 4). Additionally, the transformation level of the IR group at Week 2 was compared to those of the other groups as measured at Week 4 showed no statistically significant difference among the groups (Figure 4). Thus, callus transformation in the IR group at Week 2 was similar to that observed in the other groups by Week 4, highlighting the rapid progression of callus transformation in the IR group.

Radiological results

At Week 2, there was a statistically significant difference in callus volumes between the control and IR groups (p=0.007). The mean values were 10.69±2 mm^3 in control, 11.61±1.3 mm^3 in HA, 11.97±1.4 mm^3 in PRP and 14.36±2.1 mm^3 in IR group. At Week 4, callus volumes increased in each group; however, statistical significance of Week 2 disappeared. There was no significant difference among the groups in callus volume at Week 4 (the mean measurements for each group were 12.78±2.4 mm^3, 14.46±2.9 mm^3, 13.66±2.9 mm^3 and 15.15±2.4 mm^3 respectively, Figure 5).

At Week 2, the bone volume in the IR group was significantly higher than that in the control and PRP groups (p=0.001 and p=0.003, respectively), with mean values of 3.59±0.4 mm^3 for the control group, 4.51±0.7 mm^3 for the HA group, 3.7±0.4 mm^3 for the PRP group, and 5.21±0.5 mm^3 for the

TABLE I
The scoring table for the histologic evaluation of fracture healing

Score	Associated finding at fracture site
1	Fibrous tissue
2	Predominantly fibrous tissue with small amount of cartilage
3	Equal mixture of fibrous and cartilaginous tissue
4	Predominantly cartilage with small amount of fibrous tissue
5	Cartilage
6	Predominantly cartilage with small amount of immature bone
7	Equal mixture of cartilage and immature bone
8	Predominantly immature bone with small amount of cartilage
9	Union of fracture by immature bone
10	Union of fracture fragments by mature bone

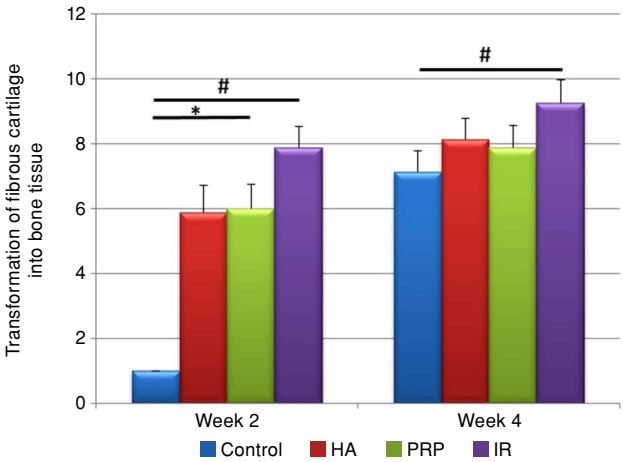

FIGURE 4. Histogram of the transformation of fibrous cartilage into bone tissue at Weeks 2 and 4.

HA: Hyaluronic acid; PRP: Platelet-rich plasma; IR: Irisin; * p<0.05; # p<0.001.

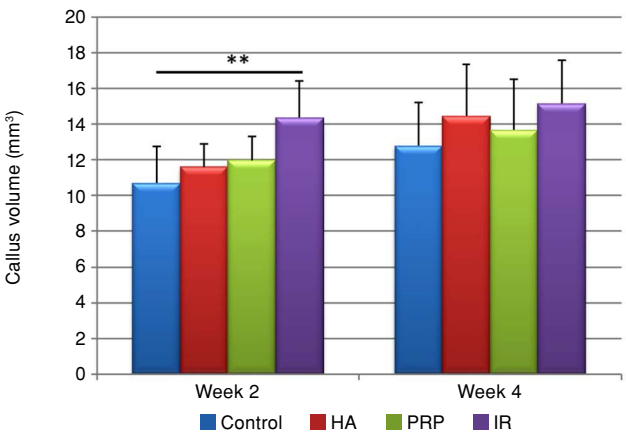

FIGURE 5. Histogram of the callus volume (mm³) at Weeks 2 and 4.

HA: Hyaluronic acid; PRP: Platelet-rich plasma; IR: Irisin; ** p<0.01.

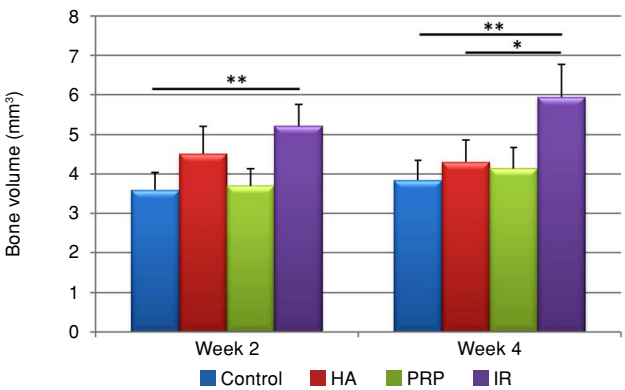

FIGURE 6. Histogram of the bone volume (mm³) at Weeks 2 and 4.

HA: Hyaluronic acid; PRP: Platelet-rich plasma; IR: Irisin; * p<0.05; ** p<0.01.

IR group. By Week 4, the mean bone volumes were measured as follows: 3.84±0.5 mm³ for the control group, 4.3±0.6 mm³ for the HA group, 4.14±0.5 mm³ for the PRP group, and 5.94±0.8 mm³ for the IR group. According to these results, the IR group exhibited the highest mean bone volume and showed statistically significant differences compared to the control group (p=0.001), the HA group (p=0.042), and the PRP group (p=0.014) at Week 4 (Figure 6).

The callus/bone volume ratio showed statistical significance only between HA and PRP groups (p=0.031) at Week 2 (3±0.6 in control, 2.6±0.3 in HA, 3.27±0.5 in PRP, and 2.77±0.4 for IR). The ratios measured at Week 4 were 3.34±0.5, 3.37±0.5, 3.41±1.1 and 2.57±0.4, respectively. The IR group had lower callus/bone volume ratio compared to other groups at Week 4. However, the p value of this comparison stayed at the significance limit (p=0.05) (Figure 7). This finding aligns with the histological observations of advanced callus transformation in the IR group.

Biomechanical testing results

The mean maximum strength levels at Week 2 were recorded as 9.79±1.4, 14±4.2, 12.38±1.6, and 27.09±7.8 Newton (N) for the control, HA, PRP, and IR groups, respectively. By Week 4, these levels increased to 28.89±9.6, 52.77±9.9, 41.79±8.8, and 75.39±10 N for the control, HA, PRP, and IR groups, respectively. The IR group showed significantly higher maximum strength compared to the control group (p=0.0001) and the PRP group (p=0.048) at Week 2. Maximum strength improved in all groups

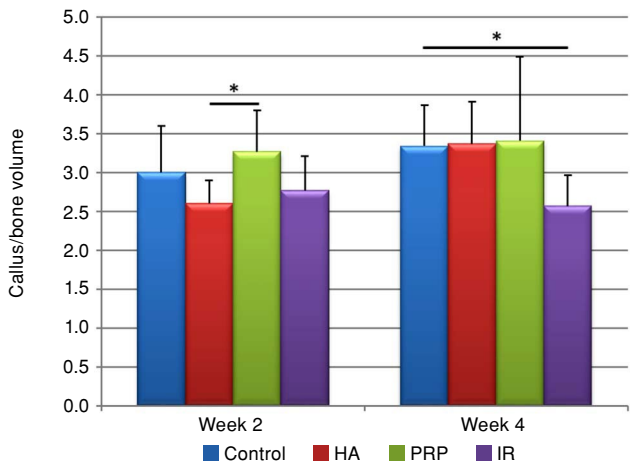

FIGURE 7. Histogram of the callus volume/bone volume at Weeks 2 and 4.

HA: Hyaluronic acid; PRP: Platelet-rich plasma; IR: Irisin; * p<0.05; ** p<0.01; # p<0.001.

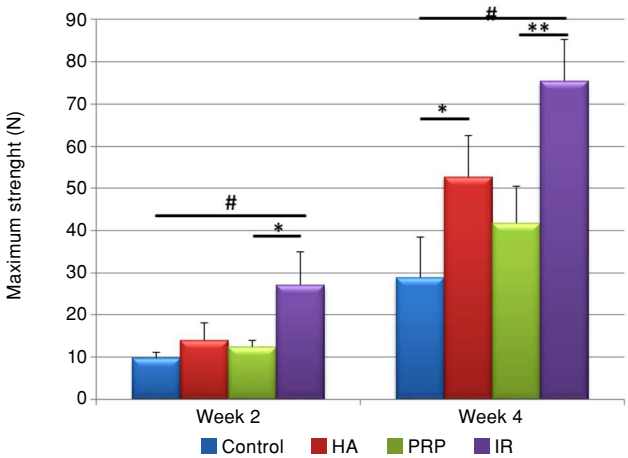

FIGURE 8. Histogram of the maximum strenght (N) at Weeks 2 and 4.
HA: Hyaluronic acid; PRP: Platelet-rich plasma; IR: Irisin; * p<0.05; ** p<0.01; # p<0.001.

by Week 4, with statistically significant differences observed between control and HA (p=0.037), control and IR (p=0.0001), and PRP and IR groups (p=0.009) (Figure 8). On the other hand, at Week 2, the mean maximum elongation levels were 1.27±0.4 mm for the control group, 1.54±0.4 mm for HA, 1.8±0.7 mm for PRP, and 2.10±1.4 mm for IR. By Week 4, these levels were 1.74±1.2, 1.3±1, 1.42±0.7, and 1.83±0.7 mm for the control, HA, PRP, and IR groups, respectively. No significant differences in maximum elongation were found among the groups at either Week 2 or Week 4.

DISCUSSION

To the best of our knowledge, the present study is among the first to investigate the effects of local IR administration via direct injection into the hematoma in a closed fracture model. Previous studies have predominantly focused on its intraperitoneal delivery.[21-23] Furthermore, the study compared local IR administration with PRP and HA, two widely used clinical methods to promote bone healing.[7-11]

The most notable finding of this study is that the average transformation of fibrous cartilage into bone tissue in the IR group at Week 2 was comparable to that of the HA and PRP groups at Week 4, with no statistically significant differences among these groups, highlighting the significant effect of IR. More intriguingly, a score of 10, indicating complete union of fracture fragments by mature bone, was observed only in the IR group, with three out of eight samples achieving this score. As these findings seem to suggest, the IR group achieved the same healing scale at Week 2 that the control, HA and PRP groups reached at Week 4. On the other hand, there was a significant difference between the PRP and control groups at Week 2, although this difference was not significant at Week 4. However, even the p value for the statistical comparison was p=0.059, no statistically significant differences were observed between the HA and control groups both for Weeks 2 and 4. To summarize, in terms of histological scoring, it was observed that while HA and PRP were effective in the transformation of callus to bone within the first two weeks, they were not as effective as IR. However, despite this positive effect, they reached the transformation scale of IR observed at Week 2 by their Week 4. By Week 4, the physiological healing process in the control group caught up with the HA and PRP groups, indicating similar transformation scores.

In biomechanical tests using the three-point bending model, the IR group exhibited significantly higher maximum strength than the control group at both Weeks 2 and 4 (p=0.0001 for both). Similarly, the IR group showed a statistically significant difference compared to the PRP group at both Weeks 2 and 4. While there was no significant difference between the HA and control groups at Week 2, a significant difference was observed at Week 4. Taken together, the IR group exhibited a significant difference compared to the control group at both Weeks 2 and 4, whereas the HA group showed a significant difference with the control group only at Week 4. There was no significant difference between the PRP and control groups at either Week 2 or Week 4. Additionally, it is noteworthy that there was no statistically significant difference between the strength values of the IR group at Week 2 and those of the control and PRP group at Week 4.

In terms of callus volume, the IR group was the only group to show a statistically significant difference compared to the control group at Week 2. However, there was no statistically significant difference between the groups at Week 4. As for bone volume, the IR group was significantly higher than both the control and PRP groups at Week 2. Regarding bone volume, at Week 2, there was a statistically significant difference between the IR group and both the PRP and control groups. At Week 4, a significant difference was observed between the IR group and all of the control, HA, and PRP groups. Although

not statistically significant, the callus/bone volume in the IR group was observed to be at the threshold of statistical significance at Week 4. This indirectly supports the notion that IR enhances the transformation of callus to bone, as indicated by histological evaluation, which resulted in an increase in radiological bone volume.

The anabolic effects of IR on bone cells have been well-documented in both *in vitro* and *in vivo* studies, demonstrating its ability to enhance osteoblast differentiation and activity while increasing osteocyte viability.[18,19] However, its effects on osteoclasts *in vitro* remain a subject of debate. Estell et al.[18] observed that IR directly stimulated osteoclastogenesis when osteoclast precursors were treated with 10 ng/mL of recombinant IR for seven days and further enhanced it at 20 ng/mL, whereas doses of 100 ng/mL or greater inhibited this process. Zhang et al.[19] reported that prolonged treatment (two months) inhibited osteoclastogenesis. Storlino et al.[20] reported that high-dose IR had catabolic effects on bone and that intermittent, lower doses, mimicking exercise, have anabolic effects. These findings emphasize the dose- and duration-dependent effects of IR.

Intraperitoneal administration of recombinant IR has been investigated in a few studies focusing on fracture healing. Colucci et al.[21] demonstrated that weekly injections of 100 μg/kg IR in mice with closed, transverse, mid-diaphyseal tibial fractures significantly enhanced endochondral ossification by Day 10 and increased callus and bone volumes by 68% and bone mineral content by 74% by Day 28, compared to controls. Similarly, Kan et al.[22] evaluated the effect of a single injection of the same dose, administered the day after surgery in a closed mid-diaphyseal femur fracture mice model. They observed improved callus formation, mineralization, and fracture healing, with elevated levels of osteogenic and angiogenic markers such as bone morphogenetic protein 2 (BMP2), VEGF, and Runt-related transcription factor 2 (Runx2). Oranger et al.[23] investigated the effects of intraperitoneal injections of the same dose, administered on Days 0 and 7 postoperatively, in a mice model with mid-diaphyseal tibial fractures, with the mice being sacrificed on Day 10. They highlighted IR's anti-inflammatory effects, reporting reductions in TNF-alpha and macrophage inflammatory protein 1 alpha (MIP-1) cytokines and increases in VEGF, BMP2, and matrix metalloproteinase-13 (MMP-13), which support vascular and matrix changes favorable for bone healing.

Local administration of IR for bone regeneration was first reported by Xin et al.[24] in 2019, who incorporated 100 ng and 200 ng of IR into a silk/calcium silicate/sodium alginate scaffold to treat 5 mm skull defects in rats. The scaffold released 50% of its IR content within seven days, promoting enhanced bone regeneration with improved mineralization after eight weeks. However, they noted that ion release (Ca and Si) from the scaffold may have contributed to bone marrow mesenchymal stem cell (BMSC) osteogenesis. In 2022, Kinoshita et al.[25] compared local IR delivery via gelatin hydrogel sheets (1.5 mm diameter, saturated with 150 ng of IR) with intraperitoneal injection in diabetic mice. Local delivery significantly improved delayed bone healing in femoral defects created with 0.8 mm drill holes, whereas intraperitoneal IR had no effect. Hua et al.[26] in 2024, evaluated poly (L-lactic acid)/HA membranes containing low (20 mg/mL) and high (200 mg/mL) doses of IR in 5 mm calvarial defects. They reported enhanced bone formation due to increased bone matrix synthesis, neo-vascularization, and the membrane's effective barrier function against soft tissue invasion. Despite these advancements, none of these studies used a closed fracture model that addressed the preservation of the fracture hematoma. If adapted clinically, these methods would likely require open surgery. In contrast, our study explored an alternative approach for administering 0.1 mL of 10 μg/mL recombinant IR directly at the fracture line under ultrasound or fluoroscopy, similar to PRP and HA applications. Moreover, while these studies employed scaffolds designed to deliver controlled and sustained release of IR, the doses of IR varied significantly and lacked comprehensive data on its dose-dependent effects. However, our study was designed to be adapted for clinical use in closed fractures with a single-dose administration, aiming to prevent infections associated with repeated injections, reduce radiation exposure from fluoroscopy, and allow for circular casting after the injection. The dosage of recombinant IR was set at 0.1 mL of a solution with a concentration of 10 μg/mL, based on the study by Serbest et al.,[28] which evaluated serum IR concentrations in fracture patients.

The main limitation to this study is that the IR treatment was administered as a single dose at a single time point. It should be evaluated for

dose- and time-dependent effects. If this could have been diversified to identify optimal dosing and timing, we might have drawn different conclusions with potentially varying results. On the other hand, the effects on the fracture were only assessed at Weeks 2 and 4. If assessments could have been made at Week 1 and Week 3 or later, and if immunohistochemical analyses had been conducted on the callus during that time, more comprehensive analyses could have been performed regarding the effect of IR on early fracture healing. Another limitation is that if serum samples had been taken prior to sacrification weeks, the serum levels of certain markers, such as osteocalcin, alkaline phosphatase, calcium, and phosphate, could have been correlated with the healing outcomes among the groups. Additionally, after creating the experimental fracture model, the fracture line should have been objectively verified as diaphyseal and non-comminuted using X-ray instead of palpation. However, the absence of comminution findings, such as butterfly fragments, in micro-CT scans, and confirmation that the fracture level was diaphyseal, indirectly suggest the reliability of the palpation method. This can be attributed to the ease of palpating the lateral and medial aspects of the rat femur and the consistency achieved by the same individual performing the procedure multiple times, despite its subjective nature.

In conclusion, this study is one of the first to investigate the effects of local IR administration via injection into the hematoma of a closed fracture model, demonstrating accelerated bone healing through earlier callus transformation and superior biomechanical strength compared to PRP and HA. These findings suggest that single-dose recombinant IR holds significant promise as a minimally invasive therapeutic approach for enhancing fracture healing, particularly in patients at risk of delayed union or nonunion, and in conservative treatments or closed surgeries such as intramedullary nailing. Nevertheless, further studies are needed to optimize dosing, timing, and evaluate its long-term effects.

Data Sharing Statement: The data that support the findings of this study are available from the corresponding author upon reasonable request.

Author Contributions: Research design, material preparation, interpretation of data, drafting the paper: A.E.A.; Material preparation and acquisition of data: A.M.E.; Revising it critically: B.Ö.; Analysis and acquisition of data: Ö.E., K.A.; Acquisition of data: T.G., H.R.B.

Conflict of Interest: The authors declared no conflicts of interest with respect to the authorship and/or publication of this article.

Funding: This study was solely supported by the Balıkesir University Scientific Research Projects Unit. No author has any professional or financial relationships that could be perceived as influencing the impartiality of the presentation.

REFERENCES

1. Clark D, Nakamura M, Miclau T, Marcucio R. Effects of aging on fracture healing. Curr Osteoporos Rep 2017;15:601-8. doi: 10.1007/s11914-017-0413-9.
2. Tzioupis C, Giannoudis PV. Prevalence of long-bone non-unions. Injury 2007;38 Suppl 2:S3-9. doi: 10.1016/s0020-1383(07)80003-9.
3. Topak D, Gürbüz K, Doğar F, Bakır E, Gürbüz P, Kılınç E, et al. Hydroxychloroquine induces oxidative stress and impairs fracture healing in rats. Jt Dis Relat Surg 2023;34:346-55. doi: 10.52312/jdrs.2023.976.
4. Önaloğlu Y, Beytemür O, Yaprak Saraç E, Biçer O, Güleryüz Y, Güleç MA. The effects of hydroxychloroquineinduced oxidative stress on fracture healing in an experimental rat model. Jt Dis Relat Surg 2024;35:146-55. doi: 10.52312/jdrs.2023.1226.
5. Kafadar İH, Yalçın Y, Çakar B. Vitamin D3 and omega-3 polyunsaturated fatty acids have beneficial effects on fracture union in an experimental rat model. Jt Dis Relat Surg 2024;35:121-9. doi: 10.52312/jdrs.2023.1397.
6. Yurteri A, Yıldırım A, Esin Çelik Z, Vatansev H, Durmaz MS. The effect of quercetin on bone healing in an experimental rat model. Jt Dis Relat Surg 2023;34:365-73. doi: 10.52312/jdrs.2023.870.
7. Meheux CJ, McCulloch PC, Lintner DM, Varner KE, Harris JD. Efficacy of intra-articular platelet-rich plasma injections in knee osteoarthritis: A systematic review. Arthroscopy 2016;32:495-505. doi: 10.1016/j.arthro.2015.08.005.
8. Jamal MS, Hurley ET, Asad H, Asad A, Taneja T. The role of Platelet Rich Plasma and other orthobiologics in bone healing and fracture management: A systematic review. J Clin Orthop Trauma 2022;25:101759. doi: 10.1016/j.jcot.2021.101759.
9. Oktaş B, Çırpar M, Şanlı E, Canbeyli İD, Bozdoğan Ö. The effect of the platelet-rich plasma on osteogenic potential of the periosteum in an animal bone defect model. Jt Dis Relat Surg 2021;32:668-75. doi: 10.52312/jdrs.2021.199.
10. Kuzuca BC, Doral MN, Mangiavini L, Sapmaz E, Maffulli N, Koken M. Investigation into the effect of epidermal growth factor and hyaluronic acid on fracture healing in a rat femoral fracture model. Acta Orthop Traumatol Turc 2023;57:229-36. doi: 10.5152/j.aott.2023.22163.
11. Akyildiz S, Soluk-Tekkesin M, Keskin-Yalcin B, Unsal G, Ozel Yildiz S, Ozcan I, et al. Acceleration of fracture healing in experimental model: Platelet-rich fibrin or hyaluronic acid? J Craniofac Surg 2018;29:1794-8. doi: 10.1097/SCS.0000000000004934.
12. Boström P, Wu J, Jedrychowski MP, Korde A, Ye L, Lo JC, et al. A PGC1-α-dependent myokine that drives brown-fat-like development of white fat and thermogenesis. Nature 2012;481:463-8. doi: 10.1038/nature10777.

13. Polyzos SA, Anastasilakis AD, Efstathiadou ZA, Makras P, Perakakis N, Kountouras J, et al. Irisin in metabolic diseases. Endocrine 2018;59:260-74. doi: 10.1007/s12020-017-1476-1.
14. Kim OY, Song J. The role of irisin in Alzheimer's disease. J Clin Med 2018;7:407. doi: 10.3390/jcm7110407.
15. Posa F, Zerlotin R, Ariano A, Cosola MD, Colaianni G, Fazio AD, et al. Irisin role in chondrocyte 3D culture differentiation and its possible applications. Pharmaceutics 2023;15:585. doi: 10.3390/pharmaceutics15020585.
16. Zerlotin R, Oranger A, Pignataro P, Dicarlo M, Maselli F, Mori G, et al. Irisin and secondary osteoporosis in humans. Int J Mol Sci 2022;23:690. doi: 10.3390/ijms23020690.
17. Zhao R, Chen Y, Wang D, Zhang C, Song H, Ni G. Role of irisin in bone diseases. Front Endocrinol (Lausanne) 2023;14:1212892. doi: 10.3389/fendo.2023.1212892.
18. Estell EG, Le PT, Vegting Y, Kim H, Wrann C, Bouxsein ML, et al. Irisin directly stimulates osteoclastogenesis and bone resorption in vitro and in vivo. Elife 2020;9:e58172. doi: 10.7554/eLife.58172.
19. Zhang J, Valverde P, Zhu X, Murray D, Wu Y, Yu L, et al. Exercise-induced irisin in bone and systemic irisin administration reveal new regulatory mechanisms of bone metabolism. Bone Res 2017;5:16056. doi: 10.1038/boneres.2016.56.
20. Storlino G, Colaianni G, Sanesi L, Lippo L, Brunetti G, Errede M, et al. Irisin prevents disuse-induced osteocyte apoptosis. J Bone Miner Res 2020;35:766-75. doi: 10.1002/jbmr.3944.
21. Colucci SC, Buccoliero C, Sanesi L, Errede M, Colaianni G, Annese T, et al. Systemic administration of recombinant ırisin accelerates fracture healing in mice. Int J Mol Sci 2021;22:10863. doi: 10.3390/ijms221910863.
22. Kan T, He Z, Du J, Xu M, Cui J, Han X, et al. Irisin promotes fracture healing by improving osteogenesis and angiogenesis. J Orthop Translat 2022;37:37-45. doi: 10.1016/j.jot.2022.07.006.
23. Oranger A, Zerlotin R, Buccoliero C, Sanesi L, Storlino G, Schipani E, et al. Irisin modulates inflammatory, angiogenic, and osteogenic factors during fracture healing. Int J Mol Sci 2023;24:1809. doi: 10.3390/ijms24031809.
24. Xin X, Wu J, Zheng A, Jiao D, Liu Y, Cao L, et al. Delivery vehicle of muscle-derived irisin based on silk/calcium silicate/sodium alginate composite scaffold for bone regeneration. Int J Nanomedicine 2019;14:1451-67. doi: 10.2147/IJN.S193544.
25. Kinoshita Y, Takafuji Y, Okumoto K, Takada Y, Ehara H, Mizukami Y, et al. Irisin improves delayed bone repair in diabetic female mice. J Bone Miner Metab 2022;40:735-47. doi: 10.1007/s00774-022-01353-3.
26. Hua X, Hou M, Deng L, Lv N, Xu Y, Zhu X, et al. Irisin-loaded electrospun core-shell nanofibers as calvarial periosteum accelerate vascularized bone regeneration by activating the mitochondrial SIRT3 pathway. Regen Biomater 2023;11:rbad096. doi: 10.1093/rb/rbad096.
27. Bonnarens F, Einhorn TA. Production of a standard closed fracture in laboratory animal bone. J Orthop Res 1984;2:97-101. doi: 10.1002/jor.1100020115.
28. Serbest S, Tiftikçi U, Tosun HB, Kısa Ü. The irisin hormone profile and expression in human bone tissue in the bone healing process in patients. Med Sci Monit 2017;23:4278-83. doi: 10.12659/msm.906293.
29. Huo MH, Troiano NW, Pelker RR, Gundberg CM, Friedlaender GE. The influence of ibuprofen on fracture repair: Biomechanical, biochemical, histologic, and histomorphometric parameters in rats. J Orthop Res 1991;9:383-90. doi: 10.1002/jor.1100090310.